The DØ Forward Proton Detector (FPD) Status[a]

Jorge Barreto - For the DØ Collaboration
Instituto de Física da UFRJ
21945-970 - Rio de Janeiro -RJ/Brazil
E-mail: barreto@if.ufrj.br

The status of the DØ Forward Proton Detector (FPD) is presented. Operational since March 2002, the FPD has being commissioned in a stand-alone data acquisition system (Sdaq) and has collected large data samples of both elastic and diffractive events. Very recently, it was integrated in the full DØ data stream, and diffractive samples have been collected. Preliminary ξ and $|t|$ distributions will be presented for these samples.

1 Introduction

Diffractive interactions account for nearly 30% of the $p+\bar{p}$ at Tevatron energy. During Run I, the DØ Collaboration has employed the Rapidity Gap (RG) technique[1-3] to studied these events. However, the RG tags might contain incertitudes, due to the existence, for instance, of underlying events destroying the gaps[4]. In order to overcome this difficulty, the DØ Collaboration has made a proposal[5] to install detectors close to the beam pipe, in order to tag both p and $\bar{p}$ scattered particle.

The forward proton detector (FPD) comprises 18 Roman Pots in 9 spectrometers. Inside each Roman Pot, scintillating fibers detectors can be brought very close to the beam. Reconstructed tracks are used to determine the momentum fraction ξ and the four-momentum transfer squared $|t|$, in an event by event base. The FPD covers the region $0 \leq t \leq 4.5$ GeV^2, with the high-$|t|$ branch never being explored before at Tevatron Energies. It can be also combined to high-p_T scattering in the central detector to measure various diffractively produced channels, as for instance, bosons W/Z, heavy flavors $b, c, J/\psi$, jets, etc.

New preliminary results from the DØ Collaboration on the subject of elastic and diffractive scattering tagged by FPD detectors will be presented.

2 The DØ Forward Proton Detector

The FPD [5,6] comprises 18 Roman Pots in 6 castles or station, as shown in Fig. 1. There are 4 stations located after the low-β quadrupole magnets, 2

[a]Invited talk presented at the 5^{th} Small-x and Diffraction Workshop, Fermilab, Batavia, Illinois, USA, September 17-20, 2003.

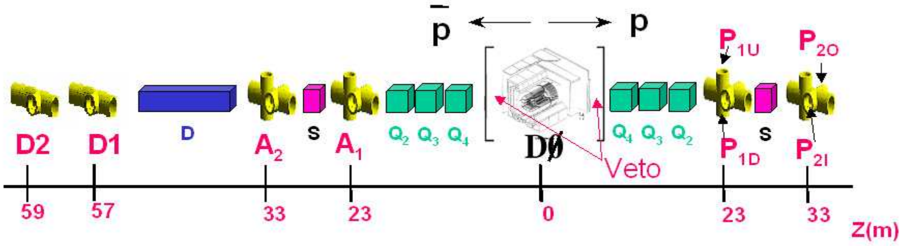

Figure 1: The FPD at DØ. Quadrupole Pots are named P or A when placed on the p or the $\bar{p}$ side, respectively. Dipole Pots, located on the $\bar{p}$ side, are named D.

of them in each side of the DØ detector, and located at $\sim 23m$ and $\sim 33m$ from the center of the detector (IP). In each of the quadrupole stations, there are 4 Roman Pots, 2 in vertical (Up, Down) and 2 in the horizontal (In,Out) positions. In the $\bar{p}$-arm there is another station after the dipole magnets, containing 1 horizontal (In) Roman Pot each, located at $\sim 57m$ and $\sim 59m$, respectively, from the IP. The system is operated by a step motor and a set of reduction gears, allowing a precision of $4-5$ microns in the pot movement. A LVDT monitors the pot positions. Constructed at Laboratório Nacional de Luz de Síncroton - LNLS/Brazil, the FPD system was installed at Fermilab during the summer of 2000, and is operating since March 2001.

Inside each Roman Pot, 3 planes (U,X,V) of scintillating fibers of width $\sim 800\mu m$ are located at the bottom of the pot (see Fig. 2). Each plane is formed of 2 layers of parallel fibers (U-U',X-X',V-V'), with the primed layers shifted by $\frac{2}{3}$ of a fiber width with respect to the unprimed ones. Inside each layer, fibers are shifted by $\frac{1}{3}$ of a fiber width, which minimizes for ghost hit problems and reduces the reconstruction ambiguities. Plane U is at $45°$ with the bottom of the pot, while planes V and X are at $135°$ and $90°$, respectively. A 200μ thick window separates the detector from the ultra high vacuum existing outside of the castle.

Scintillating fibers are spliced to clear fibers at University of Texas - Arlington/USA, to minimize for hits from halo particles, the optical cross talk in the fibers, and light attenuation, since clear fibers have an attenuation lenght longer than scintillating fibers. Each detector channel has 4 fibers each, for maximum light emission efficiency, and couples directly to a 16-channel multi-anode photomultipliers (MAPMT). There are 20 channels in each layer of the U and V planes, and only 16 channels in each of the X layers. Each detector has 112 channels and needs 7 MAPMTs, given a total of 2016 channels.

Each Roman Pot has a thick scintillating plastic trigger coupled to a PMT, that allows for a fast time signal. Signals from the DØ Luminosity Monitor

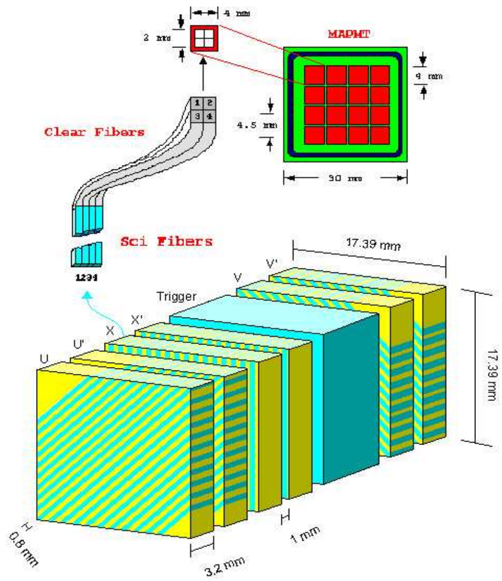

Figure 2: Detector fibers and the MAPMT.

(LM - North and South), as well as from 2 Veto Counters (VC - North and South), were also used as triggers[6].

Pot motions are controlled in the DØ Control Room via a Python program that uses the DØ online system to send commands to the step motors in the Tevatron tunnel. The software is reliable and has been tested extensively. It has many safeguards to protect against accidental insertion of the pots into the p and/or $\bar{p}$ beams. Currently, the FPD pots are inserted in every store and have accumulated large data samples on elastic and diffractive events. In the near future, the FPD system will be inserted by an automated procedure that will taken into account, for instance, the instantaneous halo rates in each pot, as well as the DØ and CDF p- and $\bar{p}$-losses, in order to determine save insertion positions for the pots.

3 Standard Particle Identification

Any diffractively scattered particle would ideally leave a signal in all 3 planes of a particular Roman Pot, but signals in only 2 planes need also to be considered, due to detector geometry or inefficiencies. The hits in one Roman Pot must be compatible with the passage of a forward particle, *i.e.* with trajectories making an angle of less than 100 μradians with the z axis. These hits are

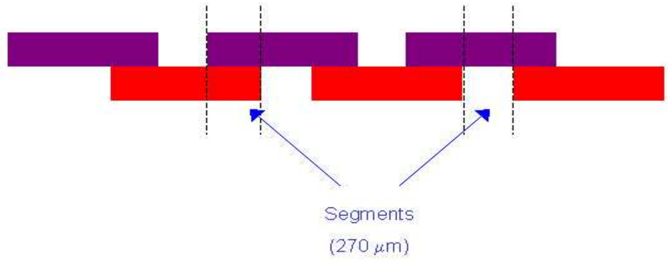

Figure 3: Hit segments.

combined in segments that can comprise one hit in each layer (*e.g.* *U-U'*) or a hit in just one of the layers of this plane (*e.g.* *U'*), as is shown in Fig. 3. This gives a total of 79 possible segments for U and V planes, and 63 for the X plane. Each segment has a width of 270 μm, giving a theoretical spatial resolution of 80 μm.

A valid track is defined only if there are hits that match in the same arm of a given spectrometer, *e.g.* PD. From the coordinates measured at each spectrometer, we can reconstruct[7] the values of the ξ, the fraction of the momentum carried by the Pomeron, and $|t|$, the four-momentum tranfer squared.

Using the FPD trigger scintillators, the Luminosity Monitor (LM), and the forward north and south scintillator veto counters (VC), an elastic trigger was setup (*Sdaq*) with only 2 distinct p and $\bar{p}$ in the event.

4 Sdaq Triggers and Elastic Events

During phase I (commissioning) of the FPD, a Stand-alone data acquisition system (Sdaq) was used to trigger on elastic and diffractive events, independently of any trigger from the DØ detector. Triggers were built with NIM logic, using signals coming from the scintillating triggers' PMTs in each of the Roman Pot, the DØ clock, the north and south veto counters, and the luminosity monitor arrays. If the event satisfied the trigger requirements, the signals coming from the fibers' MAPMTs were processed throughout CAMAC modules and saved into a PC. This configuration can read fiber informations from only 1 spectrometer (2 roman Pots), although all the trigger scintillators are available for triggering.

High-$|t|$ elastic data were obtained using a combination of vertical spectrometers in both arms. The scattered p was tagged in the PD spectrometer (P1D,P2D), while the scattered $\bar{p}$ was tagged in the AU spectrometer (A1U-A2U). The events were validated if they were on-time with respect to the DØ

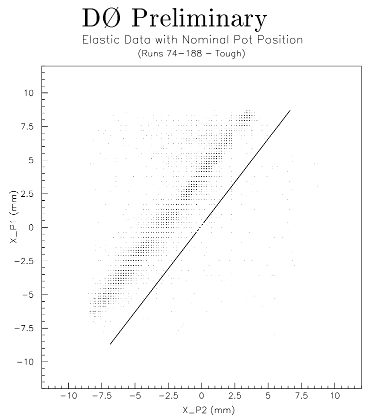

Figure 4: Elastic data (dots) and Monte Carlo simulation (line) for the correlation between nominal x positions for the hit in the spectrometer PD (se Fig.1).

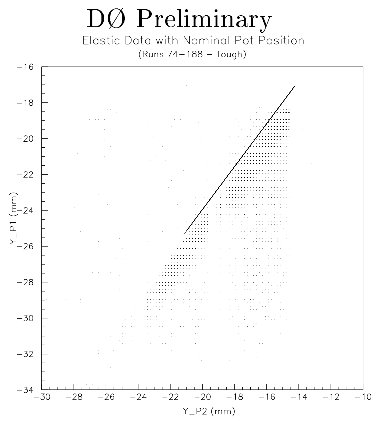

Figure 5: Elastic data (dots) and Monte Carlo simulation (line) for the correlation between nominal y positions for the hit in the spectrometer PD (se Fig.1).

DØ Preliminary

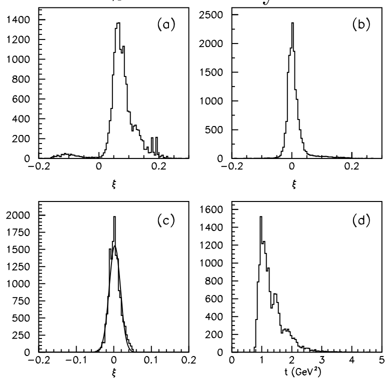

Figure 6: (a) ξ distribution before the alignment; (b) ξ distribution after the alignment; (c) fitted ξ distribution; (d) $|t|$ distribution.

clock signals, and were veto by any activity detected in the north and south parts of both LM and VC detectors, as well as by any early-time signals (halo) on any detectors of both AU and PD spectrometers. When validated by the trigger, hit fibers on P1D and P2D were read by the CAMAC modules.

Thus, over 1 million elastic events were obtained, and about 1% have passed multiplicity cuts[10], used for ease of reconstruction and to remove the background of halo spray. These events were used as input in the FPD tracking code algorithm[7–9], for the determination of the ξ and $|t|$ values. Fig. 4 shows the nominal x positions of the proton track in two different detectors of the spectrometer (P1D and P2D), while Fig. 5 shows nominal y positions correlation. When compared with results of Monte Carlo simulations, the offset of the correlations shows a misalignment of the detectors which present a relative displacement of 3mm in the x and 1mm in the y directions, respectively. The corresponding ξ distribution is shown in Fig. 6 (a), and we notice a shift with respect to $\xi = 0$, expected value for elastic events. However, when the misalignment is corrected in the tracking algorithm, a distribution that peaks at $\xi = 0$ is now obtained (see Fig. 6(b)), where the tail comes from contamination from diffractive events. If reconstructed ξ-values in the range $-0.05 \leq \xi \leq 0.05$ is only considered (Fig. 6(c)), the fitted distribution has a width 1.15 greater than the corresponding MC distribution, including smearing and dead channels. Also presented in Fig. 6(d) is the reconstructed $|t|$-distribution for the same sample of elastic events. The shape of the $|t|$-distribution is in rough agreement with MC, and it should depend only on the angular dependence of the angular acceptance of the detectors[8]. It is worth mention that the mini-

DØ Preliminary

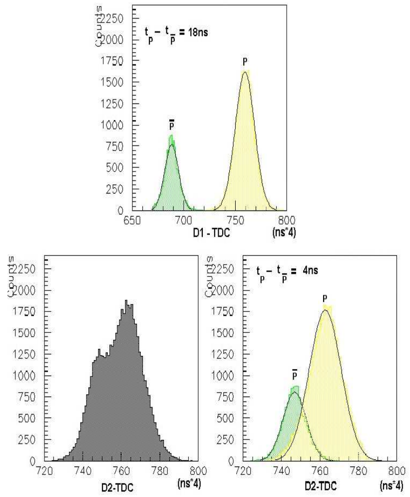

Figure 7: TDC spectra for p and $\bar{p}$ particles at locations (top): D1I; (bottom left): D2I; (bottom right): D2I gated by p or $\bar{p}$ events at D1I. Roughly, there is 0.25 ns for 1 TDC channel.

mum value of $t_{min} = 0.8\text{GeV}^2$ is determined by how close the Roman Pots are positioned from the beam.

For the dipole spectrometer DI, located at the $\bar{p}$ arm (see Fig. 1), time correlation between D1I and D2I Roman Pots is crucial, in order to obtain halo-free data samples for all diffractive events. Indeed, it takes nearly 190ns and 197ns for a scattered $\bar{p}$ to travel until D1I and D2I locations, respectively. For D2I, this time interval corresponds to the time needed for the next incoming p-bunch of the beam to travel until this location. This can be seen in Fig. 7, where TDC distributions for D1I and D2I are shown. For D1I (Fig.7-top), a clear separation between p and $\bar{p}$ halos can be observed, while both of them are merged in D2I Roman Pot (Fig.7-bottom left). Tagging upon each one of them in the D1I distribution allows to separate the merged distributions in D2I (Fig.7-bottom right).

5 The FPD in the DØ Data Stream

Since February 2003, the FPD system is integrated into the DØ data stream. To achieve this integration, signals exiting the MAPMTs were amplified and sent to a *Transition Patch Panel* - (TPP) board, that was responsible for the

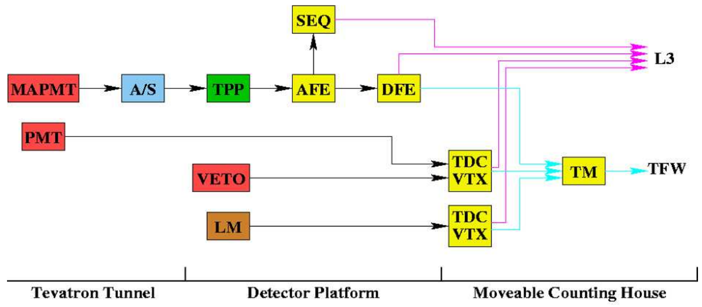

Figure 8: The FPD-DØ electronic integration schema.

matching of the analogical signals coming from the Tevatron tunnel with the *Analogical Front End* - (AFE) board, located in the DØ platform (see Fig. 8). Signals were then converted to digital and split into the *Digital Front End* - (DFE) board and into the *Sequencer board*, the former taking into account all delays necessary for matching in time all signals coming from different Roman Pots, the latter for given an appropriate signal to both *Trigger Manage* - (TM) board (L1 Trigger) and L3 Trigger.

To check if signals from MAPMTs were correctly matched and transmitted in the DØ data stream, data obtained from the AFE readout were compared[10] with data taken using the Sdaq system (see Section 4), for D1I and D2I dipole Roman Pots. In the former case, one jet with 25 GeV in the calorimeter was required in the trigger, together with no activity in the north side of the luminosity counters. In the latter, no TDC cuts were used, which would imply in a large p-halo contamination of the sample. Indeed, this is what is observed, as shown in Fig. 9, where x and y hit correlations[b] are shown. Diffracted $\bar{p}$ fall in the upper y correlation plot, while $p + \bar{p}$ halos are presented in the lower correlation seen in the y plot.

Results obtained using the AFE signals are presented in Fig. 10. It is clear that the trigger required for these events is able to suppress most of the contaminations coming from halo particles, although few of them are still observed. However, diffracted $\bar{p}$ seem to be not affected by the trigger, since they are presented in the y correlation upper plot.

The actual dipole Roman Pot insertion locations ($\sim 14\sigma$) prevents any

[b] With respect to detector fiber frames, somehow similar to the correlations shown in Figs. 4 and 5

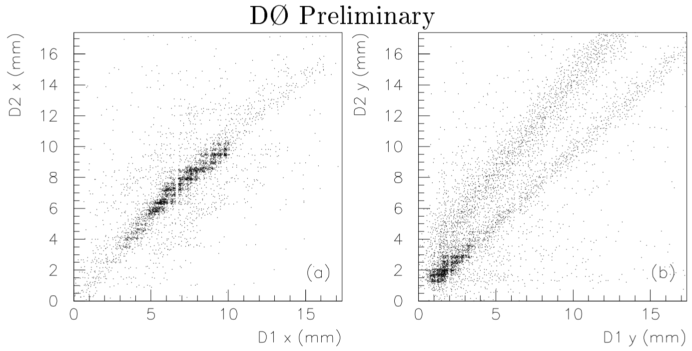

Figure 9: Sdaq x and y correlations for diffractive events in DI spectrometer.

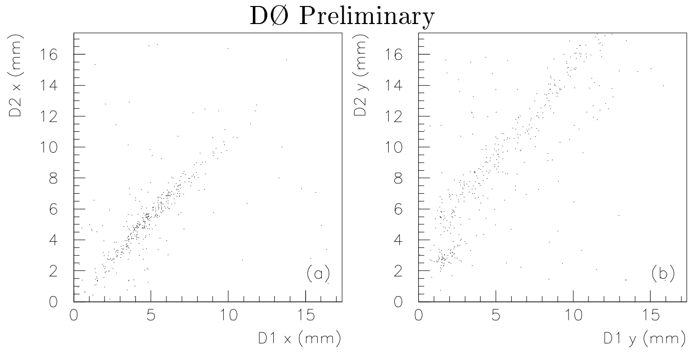

Figure 10: FTE x and y correlations for diffractive events in DI spectrometer.

measurement of elastic events, since there is no geometrical acceptance (see Fig. 13) for elastic (ξ=0) at these locations. Thus, the alignment must be done using diffractive data. Since the AFE integration seems to be performing well, we can use this diffractive data sample to perform alignment studies in the dipole spectrometer. This is shown in Fig. 11 (top), where hit (x,y) pattern are shown for both D1I and D2I Roman Pots at their nominal locations. Since the $\bar{p}$ beam is located at x=y=0, there is a clear shift in the y coordinates for both Roman Pots, whose magnitude (~ -2 mm) can be obtained (see Fig. 12) by comparing data with Monte Carlo simulations[7]. Correlations are also presented in Fig. 11 (middle), where diffracted $\bar{p}$ are clearly observed, together with some halo contaminations. Poorly reconstructed ξ and $|t|$ distributions are presented in the bottom part of Fig. 11, where the ξ distribution has a large peak at (unphysical!) negative values, which is associated to the blob of halo particles clearly seen at $x_2 > -14$ mm (see Fig.11 (middle)). The $|t|$ distribution does not show an exponential behavior, as one would expected for diffractive events. However, when the shifts $\Delta y = -2$ mm are correctly taken into account in the tracking algorithm, fair ξ and $|t|$ distributions are now obtained, as shown in Fig. 12, although halo particles contaminations seems still present in the data sample. This can be enlightened by comparing data and MC $\xi \times |t|$ correlation, as shown in Fig. 13 for MC and in Fig. 14 for data. In the Monte Carlo simulation, a flat-t input distibution was used, to give an ideia about the geometrical acceptance of this spectrometer. From this comparison, it is clear that a somewhat clean sample of diffracted events is measured at high-ξ ($0.04 \leq \xi \leq 0.06$), low-$|t|$ ($0 \leq t \leq 0.1$) range, and that another not so clean sample is measured at low-ξ, high-$|t|$ range, in which halo-particles dominate at the low-$|t|$ borne. Further analysis are under way, applying more stringent cuts, in order to obtain cleaner samples of dipole diffractive data in the integration schema.

The DØ Collaboration has recently published[11] results on the diffractive production of W and Z bosons, using Run I data sample in conjunction with the Rapidity Gap technique[1,2]. An attempt[12] was then made to identify diffractive $Z \to \mu\mu$ production in Run IIa data. A trigger requiring a gap (no hits in the north or south luminosity counter arrays) was used for collecting data. Offline, all cells in the calorimeter with an energy exceeding 100 MeV in the eletromagnetic layers in the rapidity range $|2.7| \leq \eta \leq |4.1|$ were used, with the sum of the their energies not exceeding 3 GeV. This energy cut, together with 0 hits in the corresponding luminosity counter was definied[12] as the signature of a rapidity gap on that side of the calorimeter. A dimuon system was searched in the DØ muon chambers, and the invariant dimuon mass was reconstructed, after subtracting for cosmic rays background. A few candidate

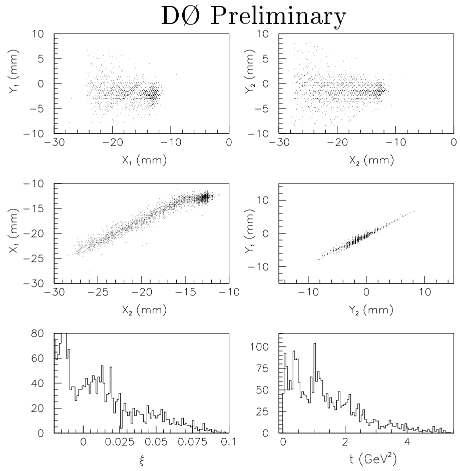

Figure 11: Event characterizations for D2I and D1I at their nominal positions. Upper: hit (x,y) patterns in D2I and D1I Roman Pots; middle: x and y correlations; bottom: ξ and $|t|$ distributions.

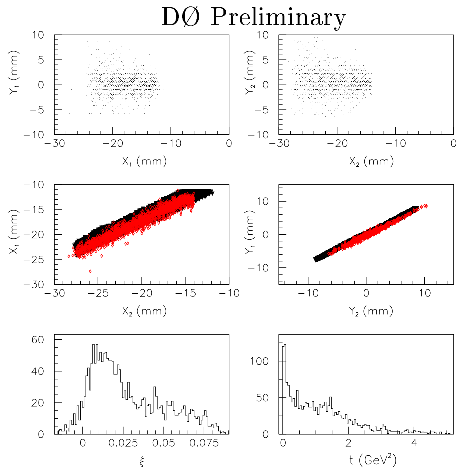

Figure 12: Event characterizations for D2I and D1I at their corrected positions. Upper: hit (x,y) patterns in D2I and D1I Roman Pots; middle: x and y correlations; bottom: ξ and $|t|$ distributions.

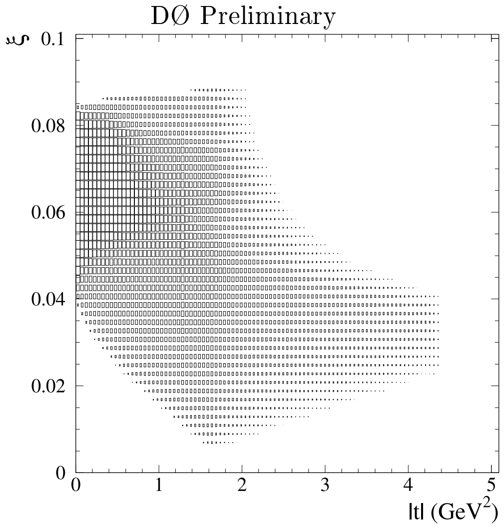

Figure 13: Monte Carlo dipole geometrical acceptance $\xi \times |t|$ obtained with a flat-$|t|$ input distribution.

events were observed, with the invariant mass centered at the Z mass value. For most of them, a $\bar{p}$ track was observed in the dipole spectrometer (D1I and D2I Roman Pots), with the track laying in the upper y_1-y_2 correlation plot (see Fig.10).

6 Conclusions

The FPD, installed at Fermilab during the summer of 2000, had a first period of commissioning during the engineering run . It was taken data since March 2001 in a Sdaq configuration which was independent of the DØ detector data stream. Elastic and diffractive data were collected using standard NIM trigger logics that were built using signals from the scintillator triggers presented in each Roman Pot of the FPD array. Since February 2003, 10 full-instrumented Roman Pots were included in the DØ detector data stream, and the results presented above, concerning as well as elastic quadrupole data (SDaq) as the diffractive results observed in the dipole spectrometer DI (DØ data stream) give clear evidences of the importance of the FPD for the future of the diffractive physics. Moreover, after the current shutdown, that is supposed to finish by mid November 2003, all 18 Roman Pots will be fully instrumented, giving us hope for a bright near future of a wealth FPD diffractive data samples.

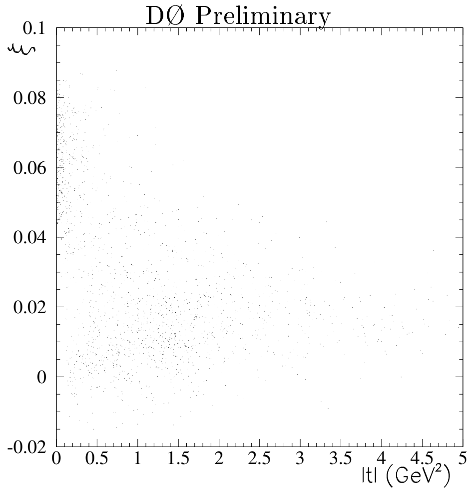

Figure 14: Dipole data $\xi \times |t|$ correlation.

7 Acknowledgments

It is a pleasure to thank all of my *FPDers* colleagues that helped in bringing the FPD system to live. I also thank the organizers of the V^{th} *Small-x Workshop* for all the financial help they gave to me, in order to present this talk.

References

1. B. Abbott *et al.* (DØ Collaboration), Phys. Lett. **B440**, (1998) 189.
2. V.M. Abazov *et al.* (DØ Collaboration), Phys. Lett. **B531**, (2002) 52.
3. J. Barreto, *DØ Results on Hard Diffraction*, Proceedings of the XXIX International Symposium on Mutiparticle Dynamics, Brown University, Providence/USA, 8-13 August 1999, edited by Ina Sarcevic and Chung-I Tang, World Scientific, pag. 283.
4. E. Gotsman, E.M. Levin and U. Maor, Phys. Lett. **B309**, (1993), 101.
5. A. Brandt et *al.*, Fermilab-Pub-97/377
6. G. Alves *et al.*, DØ Note #4054
7. J. Barreto, DØ Note #3789, DØ Note #3790
8. J. Barreto and J. Montanha, DØ Note #3791
9. V. Oguri, C. Martins and J. Barreto, *The C++ FPD Reconstruction Code I: Single Hits*, unpublised.
10. Michael Strang, private communication.
11. S. V.M. Abazov and *al.* (DØ Collaboration), hep-ph/0308032, to appear in Phys. Lett. B.
12. Tamsin Edwards, private communication.